S-Nitrosothiol Signaling Is involved in Regulating Hydrogen Peroxide Metabolism of Zinc-Stressed *Arabidopsis*

Zs. Kolbert [ID][1],*, Á. Molnár[1], D. Oláh[1], G. Feigl[1], E. Horváth[1], L. Erdei[1], A. Ördög[1], E. Rudolf[2], T. Barth[3] and C. Lindermayr [ID][2]

[1]Department of Plant Biology, University of Szeged, Szeged, Hungary
[2]Institute of Biochemical Plant Pathology, Helmholtz Zentrum München—German Research Center for Environmental Health, München/Neuherberg, Germany
[3]Research Unit Protein Science, Helmholtz Zentrum München—German Research Center for Environmental Health, München/Neuherberg, Germany
*Corresponding author: E-mail, kolzsu@bio.u-szeged.hu; Fax, +36-62-544-307.

Accumulation of heavy metals such as zinc (Zn) disturbs the metabolism of reactive oxygen (e.g. hydrogen peroxide, H_2O_2) and nitrogen species (e.g. nitric oxide, NO; S-nitrosoglutathione, GSNO) in plant cells; however, their signal interactions are not well understood. Therefore, this study examines the interplay between H_2O_2 metabolism and GSNO signaling in *Arabidopsis*. Comparing the Zn tolerance of the wild type (WT), GSNO reductase (GSNOR) overexpressor *35S::FLAG-GSNOR1* and GSNOR-deficient *gsnor1-3*, we observed relative Zn tolerance of *gsnor1-3*, which was not accompanied by altered Zn accumulation capacity. Moreover, in *gsnor1-3* plants Zn did not induce NO/S-nitrosothiol (SNO) signaling, possibly due to the enhanced activity of NADPH-dependent thioredoxin reductase. In WT and *35S::FLAG-GSNOR1*, GSNOR was inactivated by Zn, and Zn-induced H_2O_2 is directly involved in the GSNOR activity loss. In WT seedlings, Zn resulted in a slight intensification of protein nitration detected by Western blot and protein S-nitrosation observed by resin-assisted capture of SNO proteins (RSNO-RAC). LC-MS/MS analyses indicate that Zn induces the S-nitrosation of ascorbate peroxidase 1. Our data collectively show that Zn-induced H_2O_2 may influence its own level, which involves GSNOR inactivation-triggered SNO signaling. These data provide new evidence for the interplay between H_2O_2 and SNO signaling in *Arabidopsis* plants affected by metal stress.

Keywords: *35S::FLAG-GSNOR1* • Excess zincgsnor1-3 • Nitric oxide • S-nitrosoglutathione reductase • S-nitrosothiol.

Introduction

Zinc (Zn) is a nonredox metal present in soils and in surface and ground waters (Noulas et al. 2018). It is an essential micronutrient for living organisms, including plants, and it is involved in many key biological processes (Rouached 2013). Generally, agricultural soils contain 10–300 mg Zn·kg^{-1}(with an overall mean of 50–55 mg·kg^{-1}); however, the Zn content of soils can be enhanced by anthropogenic activities, including mining, industrial and agricultural practices (Kiekens 1995, Zarcinas et al. 2004).

As plants can regulate the absorption of elements within tight limits, in case of large amounts of bioavailable Zn in the rhizosphere the absorbed Zn adversely affects the life processes of plants. Plants grown in the presence of excess Zn have inward-rolled leaf edges, chlorotic leaves, and retarded and brownish root systems (Sagardoy et al. 2009, Ramakrishna and Rao 2015, Feigl et al. 2015, Feigl et al. 2016). Regarding physiological processes, elevated Zn levels result in perturbations in photosynthesis, glycolysis and electron transport due to the replacement of other divalent cations (Monnet et al. 2001, Lucini and Bernardo 2015). At the molecular level, a characteristic effect of Zn is the induction of the overproduction of reactive oxygen species (ROS) such as hydroxyl radical (·OH), superoxide radical (O_2^-) and hydrogen peroxide (H_2O_2) as reported by several studies (Weckx and Clijsters 1997, Jain et al. 2010, Feigl et al. 2015, Feigl et al. 2016). As a consequence of its redox inactive nature, Zn reportedly induces ROS production mainly through the modulation of antioxidant enzymes (e.g. Tewari et al. 2008, Wang et al. 2009) or through the formation of quinhydrone complex in the cell wall (Morina et al. 2010). The level of ROS needs to be strictly regulated by complex mechanisms, including several enzymes such as ascorbate peroxidase (APX, EC 1.11.1.11), catalase (CAT, EC 1.11.1.6), superoxide dismutase (SOD, EC1.1.5.1.1) and nonenzymatic antioxidants such as glutathione, and the activity of these antioxidant components has been shown to be affected by Zn (Cuypers et al. 2002, Di Baccio et al. 2005, Tewari et al. 2008, Gupta et al. 2011, Li et al. 2013). As a result of the Zn-triggered elevation in ROS levels, lipids, nucleic acids and proteins can be oxidized (Morina et al. 2010). Moreover, Zn stress can be accompanied by impaired DNA repair and poor protein folding (Sharma et al. 2008).

Besides ROS, reactive nitrogen species (RNS) are also overproduced as a result of a wide range of environmental stresses, including excess Zn (Feigl et al. 2015, Feigl et al. 2016). The accumulation of these nitric oxide (NO)-derived molecules principally targets proteins mainly through tyrosine nitration and S-nitrosation (Jain and Bhatla 2018). Nitration covalently modifies specific tyrosine amino acids in certain proteins, which leads to 3-nitrotyrosine formation. During the reaction, a nitro

group is added to one of the two equivalent *ortho* carbons in the aromatic ring of tyrosine residues (Gow et al. 2004), causing steric and electronic perturbations in the protein structure (van der Vliet et al. 1999). In most cases, nitration results in the inhibition of protein function in plant systems (Corpas et al. 2013). Moreover, tyrosine nitration can possibly influence signal transduction pathways through the prevention of tyrosine phosphorylation (Galetskiy et al. 2011). During S-nitrosation, RNS react with the thiol group of cysteine (Cys) resulting in the formation of an *S*-nitrosothiol (SNO) group, which in turn causes alterations in protein structure and function (Lamotte et al. 2015). So far, more than a dozen proteins have been found to be regulated either positively or negatively by S-nitrosation (reviewed by Zaffagnini et al. 2016). The S-nitrosation reaction also affects glutathione, yielding *S*-nitrosoglutathione (GSNO), which has particular relevance due to its highly stable character, its capability for being transported and its ability to liberate NO. On this basis, GSNO is considered to be a mobile reservoir of NO (Umbreen et al. 2018). The intracellular level of GSNO and, consequently, the intensity of SNO signaling are controlled by direct and selective processes like the NADPH-dependent thioredoxin reductase (NTR)–thioredoxin (TRX) system (Kneeshaw et al. 2014, Umbreen et al. 2018) and also by GSNO reductase activity (GSNOR, EC 1.2.1.1, Feechan et al. 2005, Lee et al. 2008, Chen et al. 2009). The latter enzyme catalyzes the NADH-dependent conversion of GSNO to GSSG and NH$_3$ (Jahnová et al. 2019). GSNOR is encoded by a single gene (At5g43940), and the corresponding protein was detected in the cytosol, chloroplasts, mitochondria and peroxisomes of pea leaf cells using electron microscopy immunogold-labeling technique (Barroso et al. 2013). Moreover, visualization of GSNOR-GFP in *Arabidopsis* provided clear evidence for cytosolic and nuclear localization of this protein throughout the plant (Xu et al. 2013). Regarding its protein structure, GSNOR is rich in Cys residues and contains two Zn ions per subunit, one of which has catalytic whereas the other, a structural role (Lindermayr 2018). A direct interaction between H$_2$O$_2$ and GSNOR was revealed when the H$_2$O$_2$ inducer (paraquat) triggered oxidative modification of Cys residues in the active site (Cys177, Cys47), causing release of Zn^{2+} from the catalytic site of the enzyme leading to its inactivation (Kovács et al. 2016). Additional Cys residues (e.g. Cys113 and Cys373) of GSNOR were found to be reversibly or irreversibly modified by H$_2$O$_2$. Moreover, cysteine residues allow S-nitrosation modification of GSNOR structure and activity as has been recently observed by Guerra et al. (2016). As a consequence of GSNOR inhibition, SNO accumulated and S-nitrosation intensified, suggesting a direct link between ROS and GSNO homeostasis. As the ROS overproduction can be observed during diverse environmental stresses, we can suppose that this signal interaction between ROS and RNS can be a general mechanism regulating stress responses in plants. To test this hypothesis, Zn as an environmental stressor was applied and the alterations and connections in ROS and RNS metabolism were examined. We focused our work on GSNO metabolism, using a genetic approach involving a GSNOR-deficient mutant (*gsnor1-3*) and a transgenic overproducer line (*35S::FLAG-GSNOR1*).

Results and Discussion

GSNOR-deficient line tolerates exogenous Zn better than the wild type and *35S::FLAG-GSNOR1*

Pilot experiments allowed us to select a Zn treatment (250 μM, 7 d) that was not toxic for the plant lines. As a consequence of exposure to Zn, the fresh weight of seedlings decreased in the wild type (WT) and the GSNOR overproducer line but was not influenced in *gsnor1-3* (**Fig. 1A**). However, it has to be noted that the *gsnor1-3* mutant shows multiple developmental arrests compared with the WT (**Fig. 1C**, Lee et al. 2008, Holzmeister et al. 2011, Kwon et al. 2012). The semidwarf phenotype of *gsnor1-3* indicates that GSNOR-dependent NO removal is necessary for optimal development. In the case of the WT and *35S::FLAG-GSNOR1* plants, the tolerance index decreased by the effect of Zn (**Fig. 1B, C**), which together with reduced biomass indicates Zn sensitivity. Moreover, the most significant Zn-triggered biomass loss (44%) and root shortening (20%) were observed in the GSNOR overexpressor line (**Fig. 1A–C**). Interestingly, the Zn tolerance index of *gsnor1-3* was increased, which suggests the relative Zn tolerance of this mutant. Similarly, the *gsnor1-3* mutant shows the selenium and copper tolerance (Lehotai et al. 2012, Pető et al. 2013), although in the case of this mutant impaired disease resistance and reduced heat tolerance have been observed (Feechan et al. 2005, Lee et al. 2008). This implies the possibility that the role of SNO signaling can regulate stress responses positively or negatively depending on the nature of the stress.

Zn accumulation and its root-level distribution are similar in all plant lines

In order to examine whether the different Zn tolerances of the lines are associated with different Zn accumulation capacities, Zn levels were detected in situ and in vivo. All three plant lines were able to take up Zn from the medium, which was confirmed by the elevated Zn-specific fluorescence in both the meristematic and the differentiation root zones (**Fig. 2**). Possibly due to its less active root meristem, *gsnor1-3* accumulated less Zn in this part of the root (**Fig. 2B**). The upper root part being more important in Zn uptake, the degree and magnitude of Zn accumulation therein proved to be similar in *gsnor1-3*, WT and *35S::FLAG-GSNOR1* roots (**Fig. 2**), suggesting that the reason for the relative Zn tolerance of *gsnor1-3* is not the low Zn uptake capacity.

Zn negatively regulates GSNOR activity without decreasing protein abundance and gene expression

As expected, under control conditions, both GSNOR activity (**Fig. 3A**) and protein abundance (**Fig. 3C**) were elevated in the overexpressor *35S::FLAG-GSNOR1* line and reduced in the *gsnor1-3* line relative to the WT. Excess Zn resulted in the significant reduction of GSNOR activity in the WT and caused a highly significant activity loss in the *35S::FLAG-GSNOR1* line, which was comparable with the effect of the GSNOR mutation (**Fig. 3A**). The decrease in GSNOR activity was not
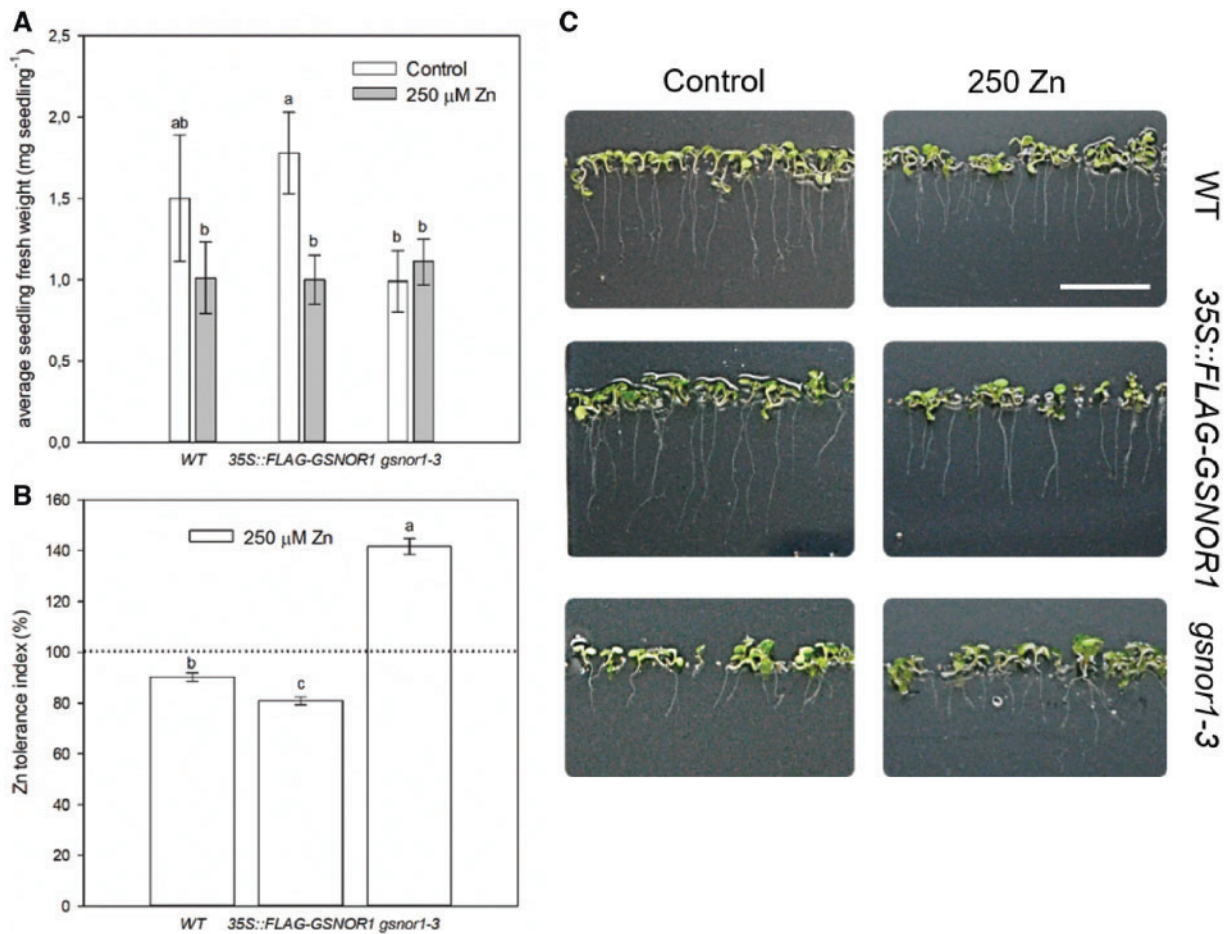
Fig. 1 Zn tolerance of *Arabidopsis* seedlings. (A) Average seedling fresh weight of 7-day-old WT, *35S::FLAG-GSNOR1* and *gsnor1-3* plants grown without (control, 15 μM) or with 250 μM Zn. (B) Zn tolerance indexes (% of control) of 250 μM Zn-treated *Arabidopsis* lines. These data were obtained from three independent replicates. Different letters indicate significant differences according to the Duncan's test ($P \leq 0.05$). (C) Representative images showing 7-day-old control and 250 μM Zn-treated WT, *35S::FLAG-GSNOR1* and *gsnor1-3 Arabidopsis*. Bar = 1 cm.

accompanied by the reduction in protein abundance, suggesting that most of the GSNOR enzyme pool present in the Zn-treated plant may be inactive. The relative transcript level of *GSNOR1* was not influenced by Zn treatment in the WT or in the mutant lines (**Fig. 3B**), indicating that the Zn-induced changes in GSNOR activity may occur at the posttranscriptional level.

SNO levels are regulated by the NADPH-dependent thioredoxin reductase system in Zn-treated *gsnor1-3*

Compared with the WT, the NO level in *35S::FLAG-GSNOR1* roots was two times higher (**Fig. 4A**), which can be explained by the higher nitrate content and increased nitrate reductase activity of this line (Frungillo et al. 2014). As a consequence of GSNOR overproduction, the SNO levels of *35S::FLAG-GSNOR1* were lower than those in the WT seedlings under control conditions (**Fig. 4B**). Both the NO and SNO levels of WT plants were increased by Zn, indicating intensified S-nitrosation processes. Zn treatment caused decreased NO levels in the root of GSNOR overexpressor *35S::FLAG-GSNOR1*, but the resulting NO content was comparable with the NO level of the Zn-treated WT plants. As for the SNO levels, those increased in Zn-exposed *35S::FLAG-GSNOR1* seedlings similarly to the WT. Several processes can be hypothesized in the background of Zn-induced NO level changes. Zn-induced iron deficiency can be partially responsible for NO production in *Arabidopsis* seedlings, as observed in *Solanum nigrum* root tips (Xu et al. 2010). A further possibility for NO production in this system is the metal-triggered decomposition of GSNO, but this remains to be elucidated. The roots of the control *gsnor1-3* mutant showed increased NO level (**Fig. 4A**) and slightly elevated total SNO level (**Fig. 4B**) as compared with the WT, which may be the result of the >80% GSNOR activity loss (Lee et al. 2008, **Fig. 3A**). Zn did not affect NO or SNO levels in the *gsnor1-3* mutant, which is interesting because, in the absence of GSNOR activity, a GSNOR-independent mechanism is necessary to prevent SNO and NO production. Besides GSNOR, the NADPH-NTR-TRX system has been considered as direct and selective denitrosylases (Umbreen et al. 2018) maintaining low SNO levels and thus temporally and spatially limiting SNO signaling.
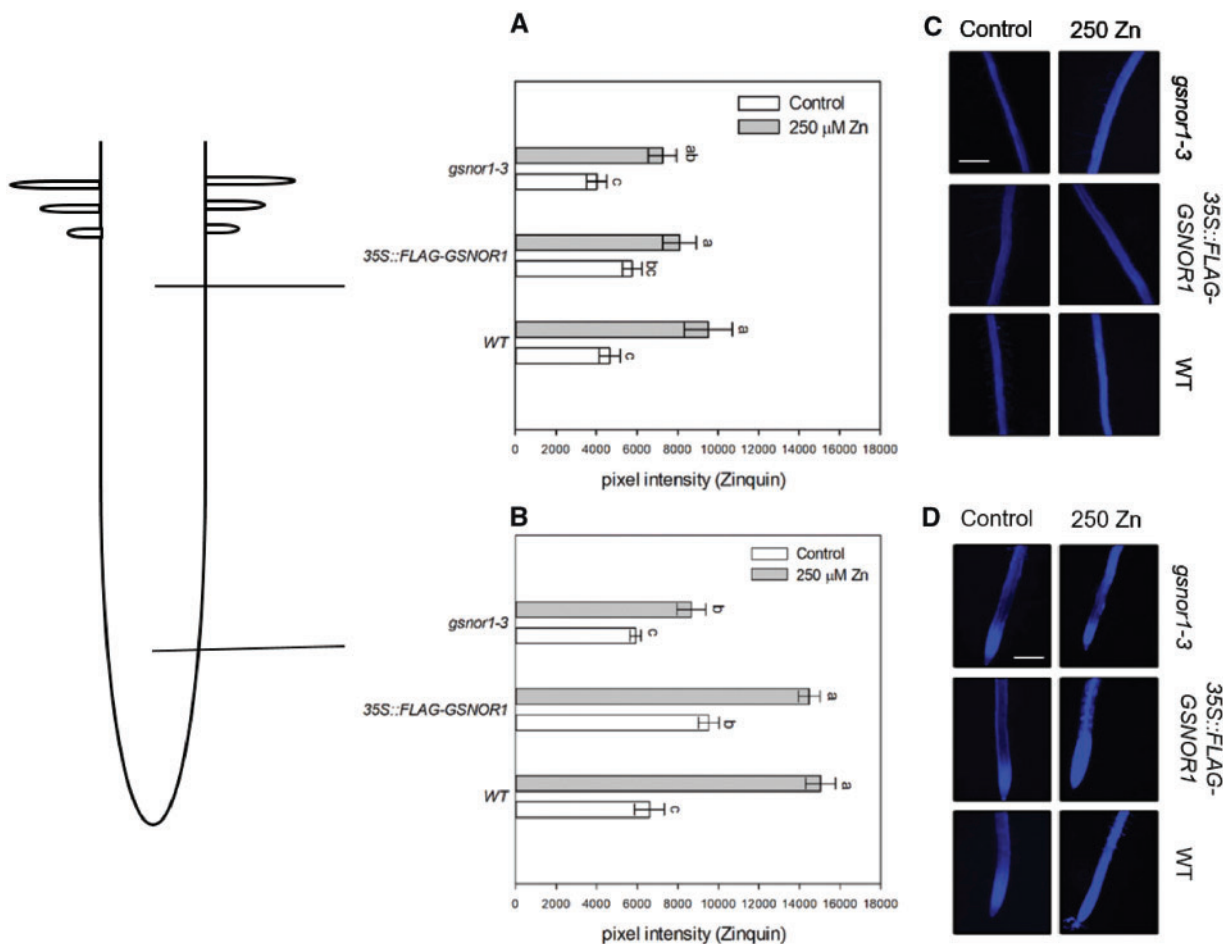
Fig. 2 Zn accumulation of *Arabidopsis* seedlings. Zn levels (estimated by Zinquin staining) in the differentiation zone (A) and meristematic region (B) of primary roots in control and 250 µM Zn-treated *WT, 35S::FLAG-GSNOR1* and *gsnor1-3* plants. These data were obtained from three independent replicates. Different letters indicate significant differences according to the Duncan's test ($P \leq 0.05$). (C, D) Representative images showing Zinquin-stained segments of the primary roots (differentiation zone, C and root tip, D). In total, 30 roots were examined. Bars = 500 µm.

Therefore, the NTR-TRX system is a good candidate for preventing Zn-induced NO/SNO level increase in the case of GSNOR deficiency. Indeed, Zn increased the activity of NTR in *gsnor1-3* seedlings (**Fig. 4C**). In addition, in the WT and *35S::FLAG-GSNOR1* lines NTR activity was lowered by Zn exposure, which together with Zn-triggered GSNOR inactivation contributes to the intensification of SNO signaling. Examining the expression of *TRX*s (**Fig. 4D**), we found that the expression of *TRXh3* was induced by Zn in the WT but not in the other lines, and Zn did not influence the expression of *TRXh5* in any of the examined *Arabidopsis* lines (data not shown). However, it cannot be excluded that TRX activity is regulated posttranscriptionally in Zn-stressed plants. These data collectively suggest that Zn may intensify SNO signaling in the WT and the GSNOR overproducer line, whereas in the case of GSNOR deficiency the induction of NTR activity may be involved in limiting SNO signaling in the presence of Zn.

Zn induces S-nitrosation in WT *Arabidopsis* seedlings

The enhancement of total SNO levels predicted the possible intensification of protein S-nitrosation in Zn-treated *Arabidopsis*. Therefore, protein extracts derived from three, independently grown sets of WT *Arabidopsis* seedlings were subjected to the resin-assisted capture of SNO proteins (RSNO-RAC) method in order to compare the rate of S-nitrosation in the seedlings grown in the presence of optimal or supraoptimal Zn supply. To verify the method, the protein extract was incubated in the presence of GSNO with the addition of Asc (**Fig. 5A**). In this sample, a remarkable enrichment of SNO proteins was observed, whereas in the absence of Asc much less SNO proteins were detected (**Fig. 5A**). These controls confirm for the first time the usability of the method for detecting SNO proteins in plant systems. Regarding the Zn effect, a slightly intensified S-nitrosation could be detected compared with the control conditions (**Fig. 5A**, arrows) possibly due to the moderate nature of Zn exposure (250 µM). To identify protein candidates for Zn-induced S-nitrosation, the samples were analyzed by LC-MS/MS. In case of GSNO treatment (in vitro S-nitrosation), 69 protein candidates were identified (Supplementary Table S2), whereas in vivo S-nitrosation in control seedlings affected 26 proteins (Supplementary Table S3). The relatively large dispersal of the data of biological replicates (**Table 1**) can be explained by the complex nature of the
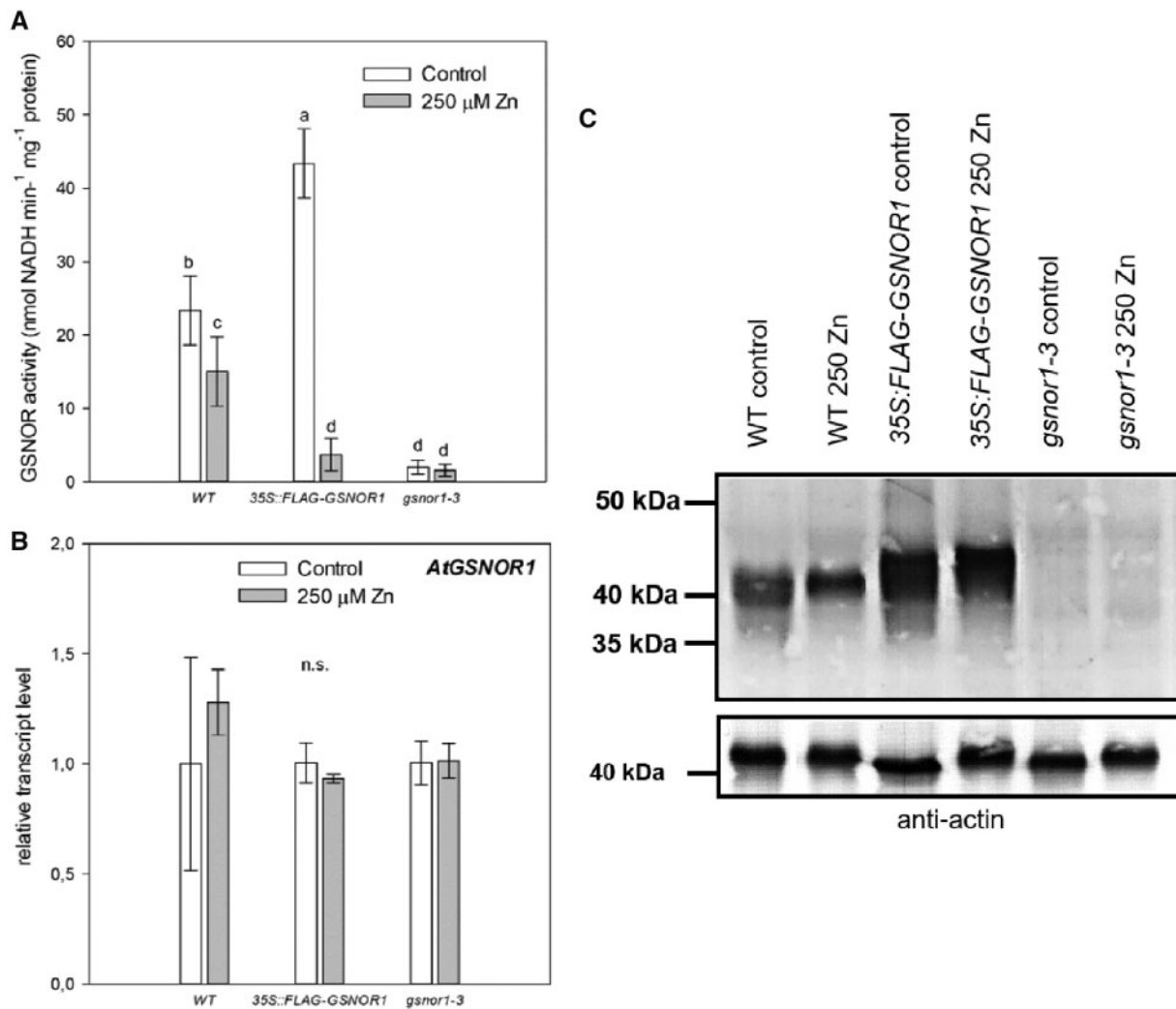
Fig. 3 Zn affects GSNOR activity, protein and transcript level in *Arabidopsis* seedlings. Activity (A) of GSNOR enzyme and relative transcript level (B) of *GSNOR1* gene in control and Zn-treated WT, *35S::FLAG-GSNOR1* and *gsnor1-3* seedlings. Data of transcript levels were normalized using the *A. thaliana ACTIN2* and *GAPDH2* genes as internal controls. The relative transcript level in control samples was arbitrarily chosen to be 1. These data were obtained from two independent replicates. Different letters indicate significant differences according to the Duncan's test ($P \leq 0.05$). (C) GSNOR protein abundance in WT, *35S::FLAG-GSNOR1* and *gsnor1-3* seedlings grown under control conditions or in the presence of 250 μM Zn. Western blot with anti-actin is shown as loading control. Band intensities were measured using GelQuant software and the data are presented as Supplementary Fig. S1.

RSNO-RAC method and by the fact that seedlings were grown in three separate experiments. Ten proteins displayed an enrichment (+Asc/−Asc ratio >1.5) in all three biological replicates making them promising candidates for S-nitrosation. However, this has to be confirmed in further experiments, e.g. using recombinant proteins. Nevertheless, the similar tendencies of biological replicates support that in Zn-treated seedlings, these 10 proteins might be S-nitrosated (**Table 1**). Among them, the S-nitrosation of APX1 was induced exclusively by the presence of Zn. According to the literature, the S-nitrosation modification of APX1 occurs at Cys32 and leads to the activation of the enzyme (Begara-Morales et al. 2014, Yang et al. 2015). In case of measuring the total activity of APX isoforms, however, we observed significant (~40%) Zn-induced activity loss (**Fig. 5B**). Moreover, 250 μM Zn treatment caused decrease

in APX protein level of WT and *gsnor1-3* seedlings, whereas in GSNOR-overproducer plants it seemed to be less modified (**Fig. 5D;** Supplementary Fig. S2). These suggest that Zn affects APX activity by lowering protein content in WT and GSNOR-deficient plants; however, GSNOR overproduction prevents the loss of APX protein level and causes inactivation without significantly influencing protein abundance.

Catalase (CAT 3) was identified as a target for S-nitrosation in GSNO-treated samples (Supplementary Table S2), therefore, the total activity of isoforms was measured in control and Zn-treated seedlings (**Fig. 5C**). Zn reduced CAT activities in all three plant lines; however, in case of *gsnor1-3*, the activity loss was not statistically significant. It is worth noting that control *35S::FLAG-GSNOR1* seedlings had 4-fold CAT activity compared with the WT (**Fig. 5C**) suggesting an effective H_2O_2
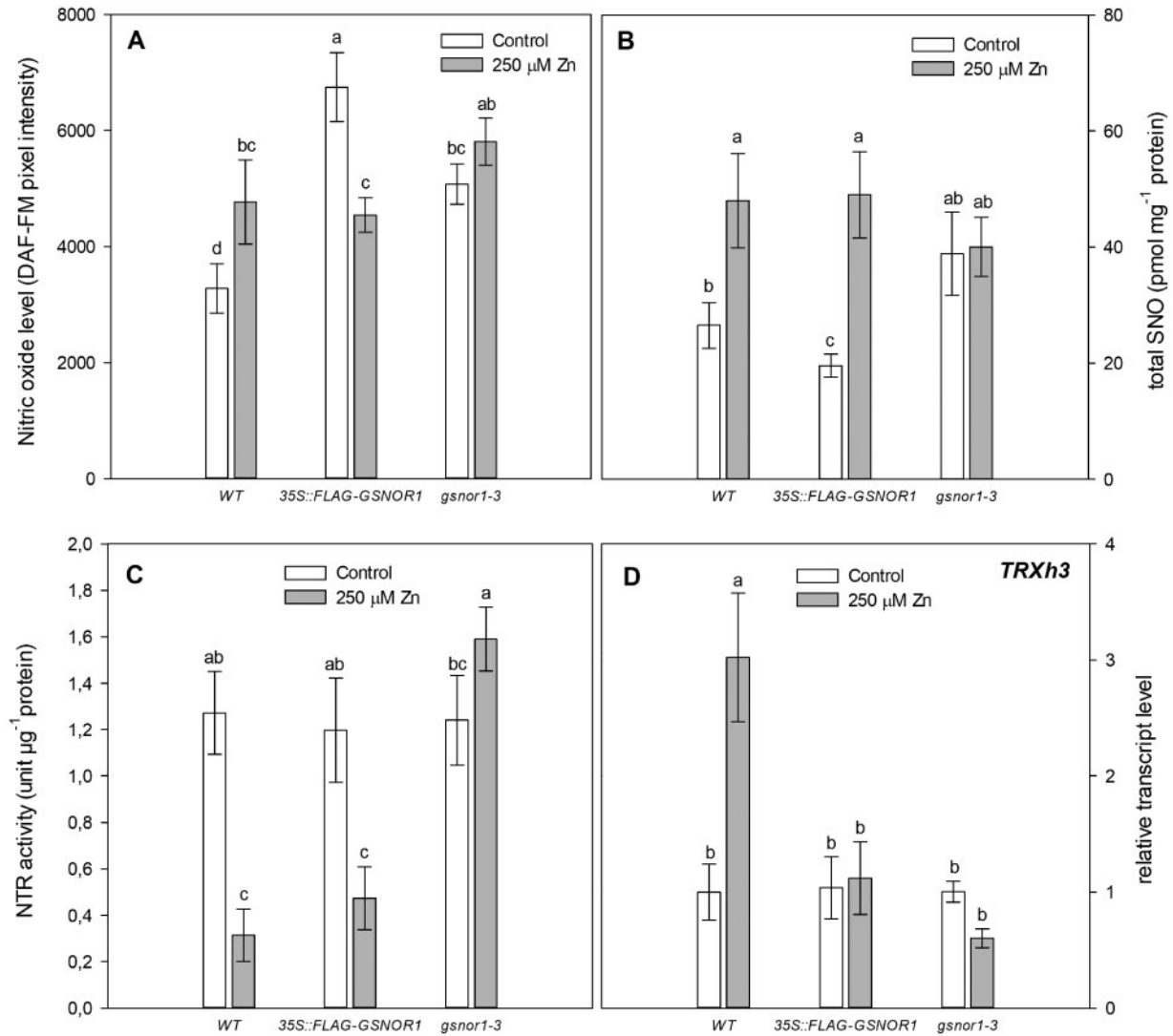
Fig. 4 NO and SNO levels are differentially affected by Zn in the *Arabidopsis* GSNOR mutants. Nitric oxide levels (A) in the root tips and SNO levels (B) in whole seedlings of WT, *35S::FLAG-GSNOR1* and *gsnor1-3* treated with Zn or grown under control conditions. (C) NADPH-dependent thioredoxin reductase (NTR) activity in control and Zn-treated *Arabidopsis* seedlings. (D) Relative transcript levels of *TRXh3* gene in WT, *35S::FLAG-GSNOR1* and *gsnor1-3* grown in the presence or absence (control) of excess Zn. Data of transcript levels were normalized using the *A. thaliana* ACTIN2 and GAPDH2 genes as internal controls. The relative transcript level in control samples was arbitrarily chosen to be 1. These data were obtained from three independent replicates. Different letters indicate significant differences according to the Duncan's test ($P \leq 0.05$).

detoxification system in case of intensified SNO signaling. The reason for the significant ($\sim$40–50%) activity losses of APX and CAT may be, inter alia, protein nitration, since both enzymes have previously been shown to be nitrated (Begara-Morales et al. 2014, Chaki et al. 2015).

Zn-induced H$_2$O$_2$ is directly involved in GSNOR inactivation

In Zn-exposed plants, SNO signaling affected H$_2$O$_2$-associated enzymes (**Table 1; Fig. 5**), therefore, it could be suspected that H$_2$O$_2$ levels are modified by the presence of Zn. Indeed, Zn treatment resulted in elevated H$_2$O$_2$ levels in the root system of all three plant lines, although this induction was the most intense (9-fold) in *gsnor1-3* (**Fig. 6A**). Despite the WT-like APX and CAT activities, the GSNOR-deficient line contained only

20% of the H$_2$O$_2$ levels of the WT in its root system under control conditions. This low H$_2$O$_2$ level may be associated with the significantly (3-fold) increased total glutathione content of this line (**Fig. 6B**). Kovács et al. (2016) also observed increased glutathione content in *gsnor1-3* compared with the WT but using 3,3'-diaminobenzidine staining similar H$_2$O$_2$ levels were detected in *gsnor1-3* and the WT. It is also interesting that Zn did not modify glutathione levels in the WT and *35S::FLAG-GSNOR1* plants, but significantly decreased the relatively high glutathione content in *gsnor1-3*. Recently, direct interaction between H$_2$O$_2$ and GSNOR has been revealed: the H$_2$O$_2$ inducer paraquat caused release of Zn^{2+} from the catalytic site of GSNOR, causing activity loss of the enzyme (Kovács et al. 2016). Therefore, we examined the possibility whether Zn-induced H$_2$O$_2$ influences the activity of GSNOR in the WT and
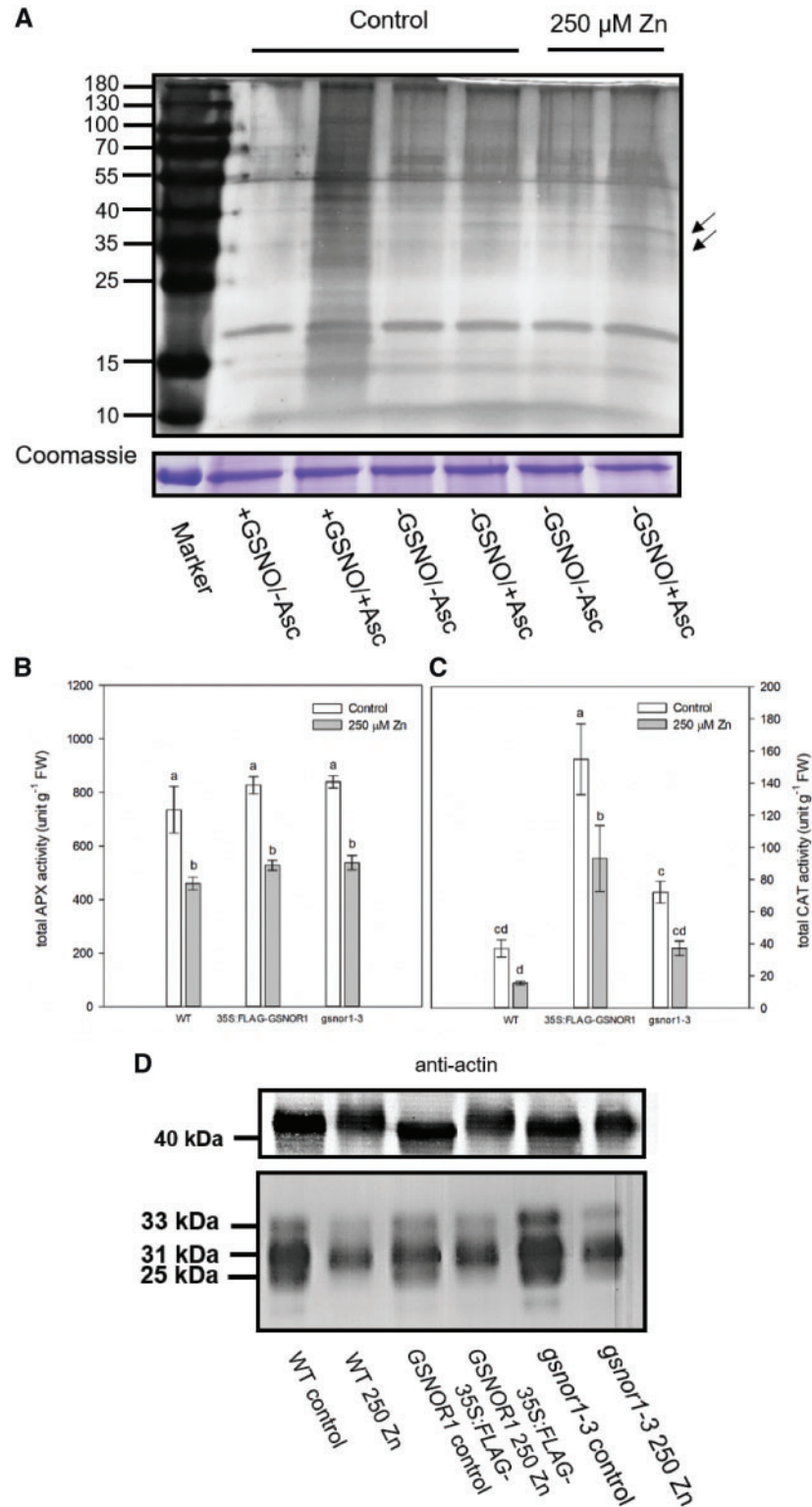
Fig. 5 Zn-induced protein S-nitrosation examined by RSNO-RAC. (A) Silver-stained SDS gel (12%) showing S-nitrosation in control and Zn-treated WT *Arabidopsis* seedlings. S-nitrosated proteins were extracted by the RSNO-RAC method. The sample homogenates treated with 1 mM GSNO served as positive control, whereas those to which ascorbate was not added served as negative controls. Input controls were visualized by Coomassie staining. Total activity of APX (B) and catalase (C) in control and Zn-treated WT, *35S::FLAG.GSNOR1* and *gsnor1-3* seedlings. These data were obtained from three independent replicates. Different letters indicate significant differences according to the Duncan's test ($P \leq 0.05$). (D) APX protein amount in control and Zn-treated WT, *35S::FLAG-GSNOR1* and *gsnor1-3* seedlings. Loading control of actin is included. Pixel densities were measured using GelQuant software and the data are presented as Supplementary Fig. S2.

Table 1 Zn-induced S-nitrosation of proteins in three sets of independently grown *Arabidopsis* seedlings (repl. 1, repl. 2, repl. 3)

Protein	kDa	Accession numbers	Number of unique peptides	Ratio +Asc/−Asc repl. 1	Ratio +Asc/−Asc repl. 2	Ratio +Asc/−Asc repl. 3
Lactate/malate dehydrogenase family protein	35	AT1G04410.1	2	10.12	66.35	5.71
L-ascorbate peroxidase 1, cytosolic	27	AT1G07890.1	3	76.55	67.63	2.66
Glyceraldehyde-3-phosphate dehydrogenase GAPC2, cytosolic	37	AT1G13440.1	5	7.25	6.87	2.27
Ribosomal protein S5/Elongation factor G/III/V family protein	94	AT1G56070.1	7	4.15	3.29	2.94
Ribosomal protein L14p/L23e family protein	15	AT1G04480.1	2	7.96	4.33	1.80
Ribosomal protein L19e family protein	25	AT1G02780.1	2	2.01	8.92	2.10
Photosynthetic electron transfer B	24	ATCG00720.1	5	2.11	5.97	1.73
Ribosomal protein L22p/L17e family protein	20	AT1G27400.1	3	5.20	8.03	1.52
Methionine adenosyltransferase 3	42	AT2G36880.1	3	5.11	3.78	1.72
Ribulose bisphosphate carboxylase small chain 1A	20	AT1G67090.1	4	6.60	2.73	1.94

Proteins were analyzed by nano-LC-MS/MS after tryptic digestion. The MASCOT search engine was used to parse MS data to identify proteins from primary sequence databases. The acquired spectra were loaded into the Progenesis QI for proteomics software (version 4.0; Nonlinear Dynamics) for MS1 intensity-based label-free quantification. Accession number: TAIR database accession number. Molecular mass in kDa. The ratio between +Asc and −Asc for each replicate is given.

in *35S::FLAG-GSNOR1*. Exogenously applied glutathione (1 mM) had no effect on control plants but resulted in decreased H$_2$O$_2$ levels in Zn-treated plants (**Fig. 6C**). Similarly, in Zn+glutathione-treated plants significantly higher GSNOR activities were measured compared with plants treated with Zn alone (**Fig. 6D**). The results indicate that the reduction of Zn-induced H$_2$O$_2$ can ameliorate GSNOR activity loss, suggesting that Zn-triggered H$_2$O$_2$ is directly involved in the inactivation of GSNOR possibly through Zn^{2+} release from the catalytic site, as described by Kovács et al. (2016). This is further confirmed by the unaffected protein abundance in Zn-treated plants (**Fig. 3C;** Supplementary Fig. S1). Moreover, a slight shift can be observed in the running of GSNOR protein in the gel (**Fig. 3C**), suggesting that Zn induces alterations in protein structure, possibly through Zn^{2+} release. At the subcellular level, Zn-induced ROS generation may occur in the apoplast (Morina et al. 2010) or in the cytoplasm as a consequence of imbalance of other essential metals (e.g. iron, Schützendübel and Polle 2002). In the cytoplasm, the GSNOR protein can be the target of ROS. Moreover, Zn can be taken up into mitochondria and chloroplasts (Nouet et al. 2011) and can induce the formation of ROS, consequently causing posttranslational modification (PTM) of the local proteins, or ROS/H$_2$O$_2$ may serve as a signal and transduce a PTM signal into the organelles.

Zn induces distinct changes in protein nitration in *Arabidopsis* lines

Nitric oxide reacts with superoxide anion to form peroxynitrite, the major RNS involved in protein nitration processes (Sawa et al. 2000). Treatment with Zn increased superoxide levels only in the roots of *35S::FLAG-GSNOR1*, whereas in the other plant lines superoxide levels remained unchanged (**Fig. 7A**). The total SOD activity decreased in Zn-treated *35S::FLAG-GSNOR1* (**Fig. 7B**), possibly contributing to the increase in the superoxide level (**Fig. 7A**). In *gsnor1-3*, a moderate increment of SOD

activity was observed, whereas Zn-exposed WT plants showed unmodified SOD activities compared with the optimal Zn supply. The activities of MnSOD and FeSOD isoforms exceeded Cu/Zn SOD activities in the control plants (**Fig. 7C;** Supplementary Fig. S4), but Zn modified this isoenzyme pattern, because it reduced the activity of FeSOD and MnSOD and increased Cu/Zn SOD activity in all three *Arabidopsis* lines. The reduced availability of Mn and Fe as an effect of excess Zn (Ebbs and Kochian 1997, Monnet et al. 2001, Feigl et al. 2016) may contribute to the decreased MnSOD and FeSOD activities. The Zn concentration applied proved to be appropriate for increasing the activity of Cu/Zn SOD due to a possible elevation of the Cu level and an increase in Zn concentration (Feigl et al. 2015, Feigl et al. 2016). Protein nitration, as the marker of nitrosative stress, has previously been shown to be increased by the effect of Zn stress (300 µM) in *Brassica* species (Feigl et al. 2015, Feigl et al. 2016). In the present system, the protein bands showing immunopositivity toward 3-nitrotyrosine antibody were detected in the low molecular weight range (16–30 kDa, **Fig. 7D**). Here, eight protein bands were selected, and the intensities of the bands were evaluated by GelQuant (Supplementary Fig. S3). In general, most protein bands showed slight Zn-induced intensification in WT and in *35S::FLAG-GSNOR1*, whereas in the GSNOR-deficient line Zn decreased the nitration of most bands. The physiological nitroproteomes of the *Arabidopsis* lines studied were similar in size, and the applied Zn concentration did not induce the appearance of newly nitrated protein bands in any of the *Arabidopsis* lines (**Fig. 7D**). In the WT, the Zn-induced mild enhancement in protein nitration may be related to the moderate production of NO and superoxide (**Figs. 4A, 7A**). In the case of *gsnor1-3*, the amount of nitrated proteins was reduced by the effect of Zn as compared with the control, which could be attributed to the activation of putative denitration processes (not yet known in plants, Kolbert et al. 2017) or by enhanced degradation of nitrated proteins.
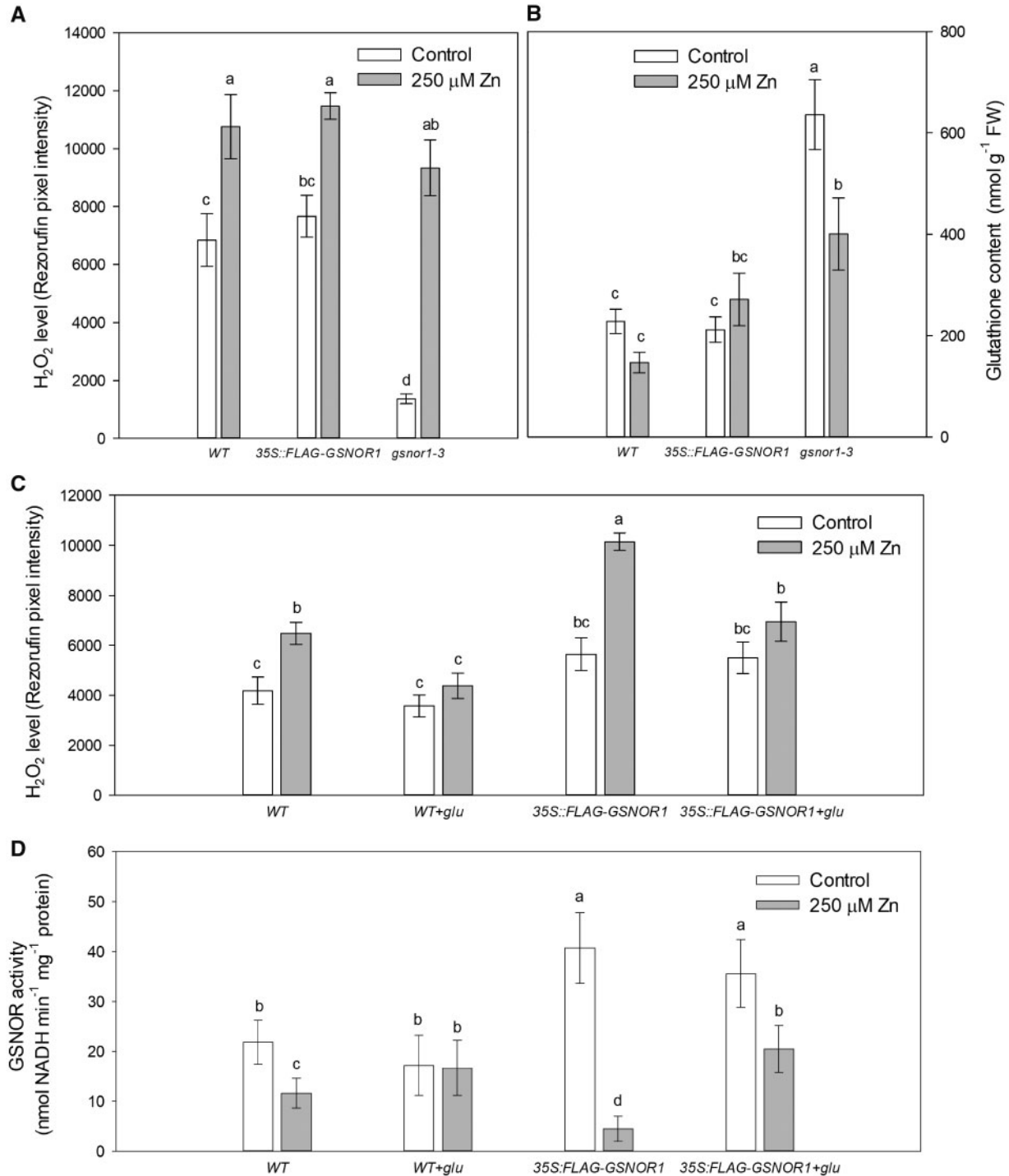
Fig. 6 Zn-induced H_2O_2 accumulation and GSNOR activity loss can be reversed by exogenous glutathione. Hydrogen peroxide levels in the root system (A) and glutathione content (B) of WT, *35S::FLAG-GSNOR1* and *gsnor1-3 Arabidopsis* grown in the presence or absence (control) of excess Zn. Hydrogen peroxide levels (C) and GSNOR activity (D) in WT, *35S::FLAG-GSNOR1* and *gsnor1-3 Arabidopsis* treated with 0 or 250 μM Zn in the absence or presence of 1 mM glutathione (+glu). These data were obtained from three independent replicates. Different letters indicate significant differences according to the Duncan's test ($P \leq 0.05$).

Conclusion

Our data collectively indicate that Zn-induced H_2O_2 is directly involved in GSNOR inactivation and it positively regulates GSNO/SNO levels, which in turn induces S-nitrosation of the APX1 enzyme. The activity changes of APX and CAT may influence H_2O_2 levels in Zn-stressed plants (**Fig. 8**). This means that Zn-induced H_2O_2 may influence its own level through a self-regulatory process which involves SNO signaling. These data provide novel evidence for the regulatory interplay between ROS (H_2O_2) and
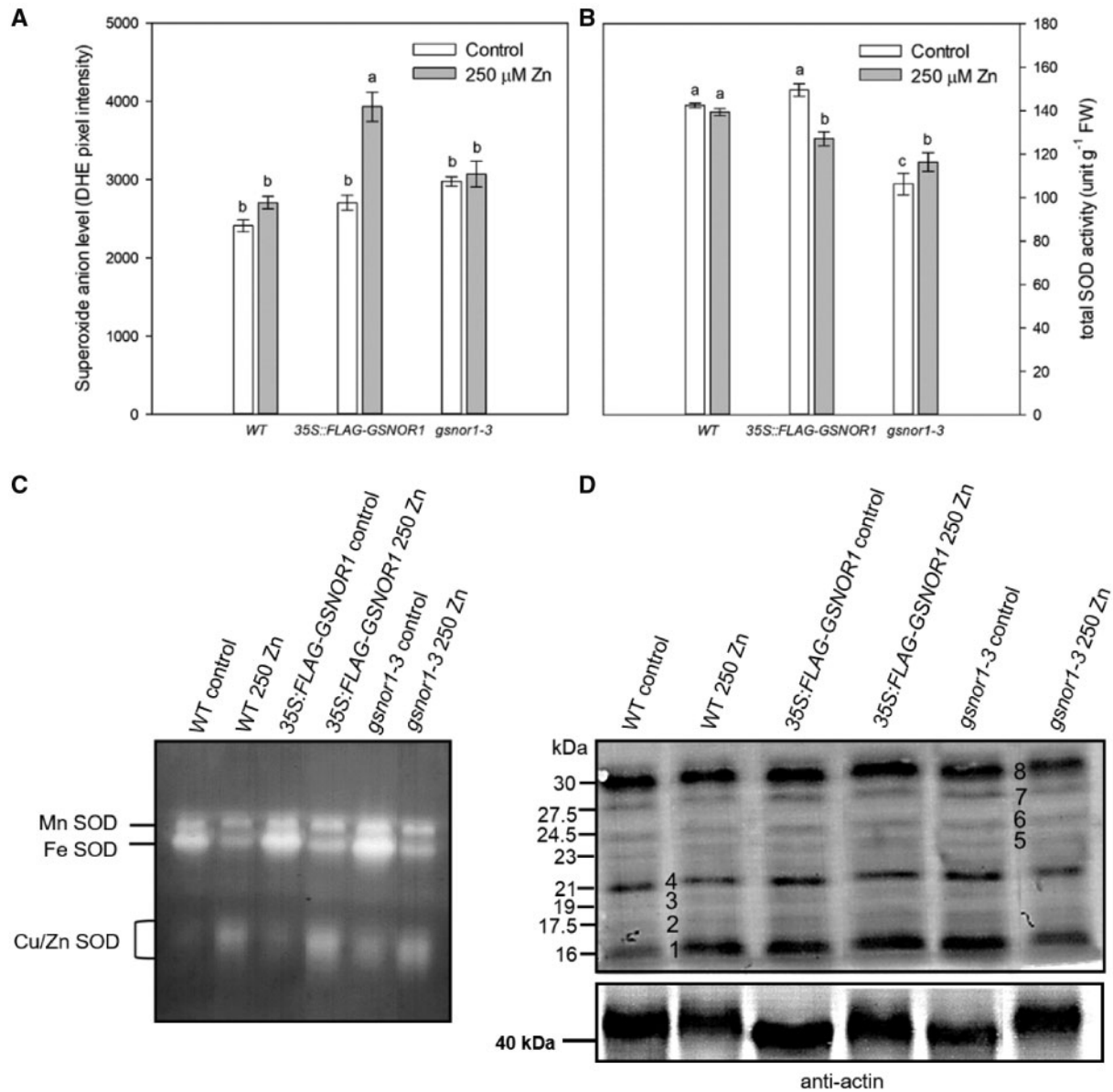
Fig. 7 Zn slightly affects superoxide metabolism and protein tyrosine nitration. Superoxide anion level in the root (A) and total SOD activity (B) in WT, *35S::FLAG-GSNOR1* and *gsnor1-3Arabidopsis* grown in the presence or absence (control) of Zn. Different letters indicate significant differences according to the Duncan's test ($P \leq 0.05$). (C) Native PAGE separation (10%) of SOD isoenzymes in control and Zn-treated *Arabidopsis* lines. (D) Western blot probed with rabbit anti-nitrotyrosine polyclonal antibody (1:2,000). Commercial nitrated BSA was used as a positive control. Loading control of actin is included. The intensities of numbered bands were quantified by Gelquant software and the data are presented as Supplementary Fig. S3. These data were obtained from three independent replicates.

SNO signaling in *Arabidopsis* plants affected by metal stress.

Materials and Methods

Plant material and growth conditions

Seven-day-old WT (*Col-0*, WT), *35S::FLAG-GSNOR1* (Frungillo et al. 2014) and *gsnor1-3* (At5g43940, Chen et al. 2009) *Arabidopsis thaliana* L. seedlings in *Col-0* background were used. The seeds were surface sterilized with 70% (v/v) ethanol and 5% (v/v) sodium hypochlorite and transferred to half-strength Murashige and Skoog medium [1% (w/v) sucrose and 0.8% (w/v) agar] supplemented with

250 μM zinc sulfate (ZnSO$_4$). In control Petri dishes, the media contained 15 μM ZnSO$_4$ as indicated by the manufacturer (Duchefa Biochemie, Haarlem, The Netherlands). The Petri dishes were kept vertically in a greenhouse at a photo flux density of 150 μmol·m^{-2}·s^{-1} (8/16 day/night period) at a relative humidity of 55–60% and 25 ± 2°C. Four days after germination, 1 mM glutathione was added on the surface of the agar containing the root system. One milliliter of glutathione solution was added per Petri dish using 2-ml syringe and sterile filter.

Evaluation of Zn tolerance

Primary root lengths were measured and from the data, Zn tolerance index (%) was calculated according to the following formula: tolerance index (%) = (treated root length/mean control root length) × 100. In addition, fresh weights of 10 seedlings were measured and the data are presented as average
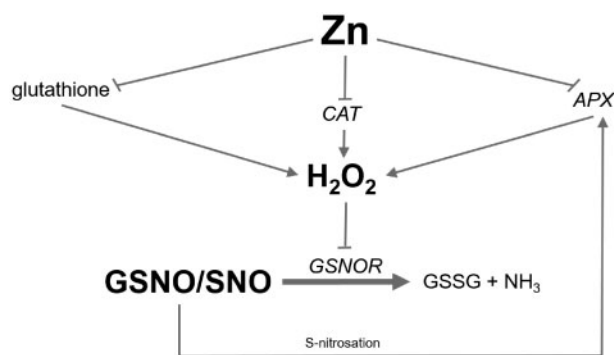
Fig. 8 Schematic model summarizing the main conclusion of this study. Excess Zn resulted in glutathione content decrease, reduced CAT and APX activities, all of which may contribute to H_2O_2 formation. Zn-induced H_2O_2 is directly involved in GSNOR inactivation, which leads to SNO accumulation and intensified S-nitrosation. We identified APX1 as a target for S-nitrosation. Based on these data, Zn-induced H_2O_2 influences its own metabolism through GSNOR inactivation-triggered SNO signaling.

seedling fresh weight (mg·seedling^{-1}). These data were acquired from three separate generations, and in each generation 20 plants were examined ($n = 20$).

Enzyme activity assays

Whole seedlings of WT, *35S::FLAG-GSNOR1* and *gsnor1-3 Arabidopsis* were ground with double volume of extraction buffer (50 mM Tris–HCl buffer pH 7.6–7.8) containing 0.1 mM EDTA, 0.1% Triton X-100 and 10% glycerol and centrifuged at $9,300 \times g$ for 20 min at 4°C. The protein extract was treated with 1% protease inhibitor cocktail and stored at −20°C. Protein concentration was determined using the Bradford (1976) assay with bovine serum albumin as a standard.

The GSNOR activity was determined by monitoring NADH oxidation in the presence of GSNO at 340 nm (Sakamoto et al. 2002). Plant homogenate was centrifuged at $14,000 \times g$ for 20 min at 4°C and 100 µg of protein extract was incubated in 1 ml reaction buffer containing 20 mM Tris–HCl pH 8.0, 0.5 mM EDTA, 0.2 mM NADH. Data are expressed as nmol NADH·min^{-1}·mg^{-1} protein.

The activity of APX was measured by monitoring the decrease of ascorbate (Asc) content at 265 nm according to the modified method of Nakano and Asada (1981). For the enzyme extract, 250 mg of plant material was ground with 1.5 ml of extraction buffer containing 1 mM EDTA, 50 mM NaCl, 900 µM Asc and 1% polyvinylpyrrolidone (PVP). Data are expressed as activity (unit·g^{-1} fresh weight).

CAT enzyme activity was measured as described by Kato and Shimizu (1987). For the enzyme extract, 250 mg of plant material was ground with 10 mg of polyvinyl polypyrrolidone (PVPP) and 1 ml of 50 mM phosphate buffer (pH 7.0, with 1 mM EDTA added). The reaction was started with the addition of 20 mM H_2O_2. The measurement itself quantifies the degradation of H_2O_2 at 240 nm and 1 unit corresponds to 1 µmol of degraded H_2O_2 per minute. The data are shown as unit·g^{-1} fresh weight.

The SOD activity was determined by measuring the ability of the enzyme to inhibit the photochemical reduction of nitroblue tetrazolium (NBT) in the presence of riboflavin in light (Dhindsa et al. 1981). The same enzyme extract was used as described previously. The enzyme activity is expressed as unit·g^{-1} fresh weight; 1 unit of SOD corresponds to the amount of enzyme causing a 50% inhibition of NBT reduction in light. For the examination of SOD isoenzyme activities, the protein extract was subjected to native gel electrophoresis on 10% polyacrylamide gel (Beauchamp and Fridovich 1971). The gel was incubated for 20 min in 2.45 mM NBT in darkness, then for 15 min in freshly prepared 28 mM TEMED solution containing 2.92 µM riboflavin. After the incubation, the gels were washed two times and developed by light exposure. SOD isoforms were identified by incubating gels in 50 mM potassium

phosphate containing 2 mM potassium cyanide to inhibit Cu/Zn SOD activity or 5 mM H_2O_2 which inhibits Cu/Zn and FeSOD activities for 30 min before staining with NBT. MnSODs are resistant to both inhibitors (Supplementary Fig. S4). To evaluate native electrophoresis, silver staining was performed according to Blum et al. (1987) with slight modifications. The gel was fixed with methanol and acetic acid, then treated with a sensitizing solution and staining solution containing AgNO₃. The gel was developed in a solution containing sodium carbonate and formaldehyde.

The activity of NTR was measured based on the method of Arnér et al. (1999) using a kit (Thioredoxin Reductase Assay Kit, Sigma-Aldrich, Merck, St. Louis, MO, USA). The manufacturer's instructions were followed during the procedure and the protein extract was prepared as described above. The measurement is based on a colorimetric reduction of 5,5′-dithiobis-2-nitrobenzoic acid (DTNB) to yellow-colored 5-thio-2-nitrobenzoic acid with NADPH. To ensure selectivity, a specific NTR inhibitor was used, and the data were validated using rat liver thioredoxin reductase as positive control. Data are shown as unit·µg^{-1} protein. These experiments were carried out on two separate plant generations with five samples in each ($n = 5$).

The measurement of total glutathione content was done according to Griffith (1980) with slight modifications. Whole seedlings were ground with 5% trichloroacetic acid, centrifuged for 20 min at $9,300 \times g$ and the supernatant was used for further measurement. The reaction mixture contained 25 µl sample, 0.1 M sodium phosphate buffer, 1 mM of DTNB, 1 mM NADPH and 1 unit of glutathione reductase enzyme. The method is based on enzymatic recycling by glutathione reductase. During the reaction, the formation rate of 5-thio-2-nitrobenzoate is directly proportional to the rate of the recycling reaction, which is directly proportional to the glutathione content. The change in absorbance (at 412 nm) during 1 min corresponds to the concentration of glutathione, using GSSG as standard. Data are shown as nmol·g^{-1} fresh weight. These experiments were carried out on two separate plant generations with five samples in each ($n = 5$).

Microscopic detection of Zn levels, NO, H_2O_2 and O_2^- in the roots

The endogenous levels of Zn were visualized by the Zn-specific fluorophore, Zinquin [ethyl (2-methyl-8-*p*-toluenesulphonamide-6-quinolyloxy)acetate (Helmersson et al. 2008)]. Seedlings were equilibrated in phosphate-buffered saline (PBS; 137 mM NaCl, 2.68 mM KCl, 8.1 mM Na₂HPO₄, 1.41 mM KH₂PO₄, pH 7.4) and further incubated in 25 µM Zinquin solution (in PBS) for 60 min at room temperature in darkness. Before the microscopic investigation, the samples were washed once with PBS buffer.

The nitric oxide levels of the root tips were monitored with the help of 4-amino-5-methylamino-2′,7′-difluorofluorescein diacetate (DAF-FM DA) according to Kolbert et al. (2012). Whole seedlings were incubated in 10 µM dye solution for 30 min (darkness, 25 ± 2°C) and washed twice with Tris–HCl (10 mM, pH 7.4).

The levels of H_2O_2 were detected by Amplex Red (AR), which in the presence of peroxidase and H_2O_2 forms highly fluorescent resorufin (Prats et al. 2008). Seedlings were incubated in 50 µM AR solution (prepared in sodium phosphate buffer pH 7.5) for 30 min at room temperature in darkness. The microscopic observations were preceded by one washing step with sodium phosphate buffer.

Dihydroethidium (DHE) at 10 µM concentration was applied for the detection of superoxide anion levels in the roots. Seedlings were incubated for 30 min in darkness at 37°C, and washed two times with Tris–HCl buffer (10 mM, pH 7.4) (Kolbert et al. 2012).

Seedlings labeled with different fluorophores were examined under Zeiss Axiovert 200 M microscope (Carl Zeiss, Jena, Germany) equipped with filter set 9 (excitation 450–490 nm, emission 515–∞ nm) for DHE, filter set 10 (excitation 450–490 nm, emission 515–565 nm) for DAF-FM DA, filter set 20 HE (excitation 546/12 nm, emission 607/80 nm) for Amplex Red or filter set 49 (excitation 365 nm, emission 455/50 nm) for Zinquin. Fluorescence intensities (pixel intensity) in the roots were measured on digital images using Axiovision Rel. 4.8 software within circles of 37-µm radii. These analyses were carried out three times with 10 samples each ($n = 10$). Controls for fluorescent probes are shown in Supplementary Fig. S5.

Determination of SNO contents

The total amount of SNO was quantified by Sievers 280i NO analyzer (GE Analytical Instruments, Boulder, CO, USA). Moreover, 250 mg of *Arabidopsis* seedlings was mixed with a double volume of 1× PBS buffer (containing 10 mM *N*-ethylmaleimide and 2.5 mM EDTA, pH 7.4) and were ground using Fast Prep® Instrument (speed 5.5; 60 s, Savant Instruments Inc., Holbrook, NY, USA). Samples were centrifuged twice for 15 min at 20,000 × *g* at 4°C each. The supernatants were incubated with 20 mM sulfanilamide (prepared in 1 M HCl) at a ratio of 9:1 in order to remove nitrite. Moreover, 250 μl of the samples was injected into the reaction vessel filled with potassium iodide. SNO concentrations were quantified with the help of NO analysis software (v3.2) by integrating peak areas and using a standard curve. The standard curve was generated by adding known concentrations of sodium nitrite. These experiments were carried out on three separate plant generations with five to seven samples examined each ($n = 5–7$).

Analysis of S-nitrosated proteins by RSNO-RAC

For the determination of S-nitrosated proteins in WT *Arabidopsis* seedlings, the method of resin-assisted capture of SNO proteins was adapted (Thompson et al. 2013). Whole seedling material (2 g) was ground in liquid nitrogen and homogenized in HENT buffer (100 mM HEPES-NaOH, pH 7.4, 1 mM EDTA, 0.1 mM neocuproine, 0.2% Triton X-100). The homogenate was centrifuged at 18,000 × *g*, 15 min, 4°C followed by another centrifugation step (18,000 × *g*, 10 min, 4°C). Protein concentration was determined according to Bradford (1976). Some of the samples were treated with 1 mM GSNO for 30 min in the darkness with multiple mixes. During the blocking step, samples were incubated with 25% sodium-dodecyl-sulfate (SDS) and 2 M S-methyl methanethiosulfonate at 50°C, at 300 rpm, for 20 min. Incubation of the samples with 100% ice-cold acetone at −20°C was followed by several washings with 70% acetone with centrifugations (5 min, 10,000 × *g*). The pellets were resuspended in HENS buffer (HEN + 1% SDS) and input controls were mixed with Laemmli 2×. Certain samples were treated with 200 mM sodium Asc for 10 min. The previously prepared Thiopropylsepharose 6B (GE Healthcare Life Sciences) beads were added to the samples and those were incubated with the beads for 2 h in the darkness with constant mixing. The beads were washed with 4 × 3 ml HENS buffer and 2 × 2 ml HENS/10 buffer. The samples were eluted with mercaptoethanol. The samples were subjected to SDS-PAGE (12%) and the gels were stained with Coomassie Brilliant Blue R-350 (input controls) or with silver (Pierce™ Silver Stain Kit, Thermo Fisher Scientific, Waltham, MA USA). These analyses were carried out on three separate plant generations ($n = 3$).

Sample preparation for MS analysis

From each of the SNO-enriched purifications, part of the eluted proteins was digested using a modified filter-aided proteome preparation procedure (Wiśniewski et al. 2009). The samples were acidified with trifluoroacetic acid and stored at −20°C.

Mass spectrometry

The LC-MS/MS analysis was performed on a Q Exactive HF mass spectrometer (Thermo Fisher Scientific) online coupled to a nano-RSLC (Ultimate 3000 RSLC; Dionex). Tryptic peptides were accumulated on a nanotrap column (Acclaim PepMap 100 C18, 5 μm, 100 Å, 300 μm inner diameter (i.d.) × 5 mm; Thermo Fisher Scientific) at a flow rate of 30 μl·min^{-1} and then separated by reversed phase chromatography (nanoEase M/Z HSS C18 T3 Column, 100 Å, 1.8 μm, 75 μm i.d. × 250 mm; Waters) using a nonlinear gradient for 95 min from 3% to 40% buffer B [acetonitrile (v/v)/0.1% formic acid (v/v)] in buffer A [2% acetonitrile (v/v)/0.1% formic acid (v/v) in HPLC-grade water] at a flow rate of 250 nl·min^{-1}. MS spectra were recorded at a resolution of 60,000 with an AGC target of 3 × 10^6 and a maximum injection time of 50 ms at a range of 300–1,500 *m/z*. From the MS scan, the 10 most abundant ions were selected for HCD fragmentation with a normalized collision energy of 28, an isolation window of 1.6 *m/z*, and a dynamic exclusion of 30 s. MS/MS spectra were recorded at a resolution of 15,000 with an AGC target of 10^5 and a maximum injection time of 50 ms. Unassigned charges, and charges of 1 and >8 were excluded. One technical replicate per biological replicate was analyzed.

Label-free analysis

The acquired spectra were loaded into the Progenesis QI for proteomics software (version 4.0; Nonlinear Dynamics) for MS1 intensity-based label-free quantification. The alignment of retention times was performed to a maximal overlay of all features. After the exclusion of features with one charge and charges >7, all remaining MS/MS spectra were exported as Mascot generic file and used for peptide identification with Mascot (version 2.6.2) with the TAIR database (Release 10, 35,386 entries). Search parameters used for Mascot search were 10 ppm peptide mass tolerance and 20 mmu fragment mass tolerance with trypsin as protease and one missed cleavage allowed. Carbamidomethylation of cysteine was set as fixed modification, methionine oxidation and asparagine or glutamine deamidation were allowed as variable modifications. Mascot integrated decoy database search was set to a false discovery rate of 5%. Peptide assignments were reimported into the Progenesis QI software. Raw protein abundances resulting from the addition of all unique peptides of a given protein group were used for calculation of +Asc/−Asc ratios [raw abundance of a distinct protein when sample was treated with Asc (+Asc) divided by the raw abundance of the same protein in the sample without Asc (−Asc) treatment] for each protein and each replicate. Proteins with a ratio higher than at least 1.2 in each replicate were defined as S-nitrosated.

Quantitative real-time PCR analysis

The expression rates of *GSNOR1*, *THIOREDOXIN-h3* (*TRXh3*) and *THIOREDOXIN-h5* (*TRXh5*) genes in *A. thaliana* were determined by quantitative real-time reverse transcription-PCR (RT-qPCR). RNA was purified from 90 mg plant material by using NucleoSpin RNA Plant mini spin kit (Macherey-Nagel, Düren, Germany) according to the manufacturer's instruction. An additional DNase digestion was applied (Thermo Fisher Scientific), and cDNA was synthetized using RevertAid reverse transcriptase (Thermo Fisher Scientific). Primers were designed for the selected coding sequences using the Primer3 software; the primers used for RT-qPCR are listed in Supplementary Table S1. The expression rates of the selected genes were monitored by quantitative real-time PCR (Jena Instruments, Jena, Germany) using SYBR Green PCR Master Mix (Thermo Fisher Scientific) as described by Gallé et al. (2009). Data analysis was performed using qPCRsoft3.2 software (Jena instruments). Data were normalized to the transcript levels of the control samples; *ACTIN2* (*At3g18780*) and *GAPDH2* (*At1g13440*) were used as internal controls (Papdi et al. 2008). Each reaction was carried out in two replicates using cDNA synthesized from independently extracted RNAs and the experiments were repeated two times.

Western blot analyses of proteins

Protein extracts were prepared as described above. Fifteen microliters of denatured protein extract was subjected to SDS-PAGE on 12% acrylamide gels. Transfer to PVDF membranes was done using a wet blotting procedure (25 mA, 16 h) and membranes were used for cross-reactivity assays with different antibodies. To evaluate the electrophoresis and transfer, we used Coomassie Brilliant Blue R-350 staining according to Welinder and Ekblad (2011). As a protein standard, actin from bovine muscle (Sigma-Aldrich, cat. No. A3653) was used and loading controls were performed using anti-actin antibody (Agrisera, cat. No. AS13 2640, Vannas, Sweden).

Immunoassay for GSNOR enzyme was performed using a polyclonal primary antibody from rabbit (Agrisera, cat. No. AS09 647) diluted 1:2,000. Affinity-isolated goat anti-rabbit IgG–alkaline phosphatase secondary antibody was used (Sigma-Aldrich, cat. No. A3687) at a dilution of 1:10,000, and bands were visualized by using the NBT/BCIP (5-bromo-4-chloro-3-indolyl phosphate) reaction.

To evaluate APX protein content, Western blot using rabbit anti-APX antibody (Agrisera, cat. No. AS 08 368) was used. As secondary antibody, similarly to the previous methods goat anti-rabbit IgG–alkaline phosphatase was used. Protein bands were developed by the NBT/BCIP reaction.

The detection of nitrated proteins was similar as described above. Membranes were subjected to cross-reactivity assay with rabbit polyclonal antibody against 3-nitrotyrosine (Sigma-Aldrich, cat. No. N0409) diluted 1:2,000. Affinity-isolated goat anti-rabbit IgG–alkaline phosphatase secondary antibody was used (Sigma-Aldrich, cat. No. A3687) at a dilution of 1:10,000, and bands were visualized by using the NBT/BCIP reaction. For positive control,

nitrated BSA (Sigma-Aldrich, cat. No. N8159) was used. Protein bands of nitrated protein, GSNOR enzyme and APX enzyme were quantified by Gelquant software (provided by biochemlabsolutions.com). The Western blot was applied to two separate protein extracts from different plant generations, multiple times per extract, giving a total of four-blotted membranes ($n = 2$).

Statistical analysis

All results are shown as mean values of raw data (±SE). For statistical analysis, the Duncan's multiple range test (one-way ANOVA, $P \leq 0.05$) was used in SigmaPlot 12. For the assumptions of ANOVA, we used the Hartley's F_{max} test for homogeneity and the Shapiro–Wilk normality test.

Supplementary Data

Supplementary data are available at PCP online.

Disclosures

The authors have no conflicts of interest to declare.

References

Arnér, E.S.J., Zhong, L. and Holmgren, A. (1999) Preparation and assay of mammalian thioredoxin and thioredoxin reductase. *Methods Enzymol.* 300: 226–239.

Barroso, J.B., Valderrama, R. and Corpas, F.J. (2013) Immunolocalization of S-nitrosoglutathione, S-nitrosoglutathione reductase and tyrosine nitration in pea leaf organelles. *Acta Physiol. Plant.* 35: 2635–2640.

Beauchamp, C. and Fridovich, I. (1971) Superoxide dismutase: improved assays and an assay applicable to acrylamide gels. *Anal. Biochem.* 44: 276–287.

Begara-Morales, J.C., Sánchez-Calvo, B., Chaki, M., Valderrama, R., Mata-Pérez, C. and López-Jaramillo, J. (2014) Dual regulation of cytosolic ascorbate peroxidase (APX) by tyrosine nitration and S-nitrosylation. *J. Exp. Bot.* 65: 527–538.

Blum, H., Beier, H. and Gross, H.J. (1987) Improved silver staining of plant proteins, RNA and DNA in polyacrylamide gels. *Electrophoresis* 8: 93–99.

Bradford, M.M. (1976) A rapid and sensitive method for the quantitation of microgram quantities of protein utilizing the principle of protein-dye binding. *Anal. Biochem.* 72: 248–254.

Chaki, M., Álvarez de Morales, P., Ruiz, C., Begara-Morales, J.C., Barroso, J.B., Corpas, F.J., et al. (2015) Ripening of pepper (*Capsicum annuum*) fruit is characterized by an enhancement of protein tyrosine nitration. *Ann. Bot.* 116: 637–647.

Chen, R., Sun, S., Wang, C., Li, Y., Liang, Y., An, F., et al. (2009) The *Arabidopsis* PARAQUAT RESISTANT2 gene encodes an S-nitrosoglutathione reductase that is a key regulator of cell death. *Cell Res.* 19: 1377–1387.

Corpas, F.J., Palma, J.M., del Río, L.A. and Barroso, J.B. (2013) Protein tyrosine nitration in higher plants grown under natural and stress conditions. *Front. Plant Sci.* 4: 29.

Cuypers, A., Vangronsveld, J. and Clijsters, H. (2002) Peroxidases in roots and primary leaves of *Phaseolus vulgaris* copper and zinc phytotoxicity: a comparison. *J. Plant Phys.* 159: 869–876.

Dhindsa, R.S., Plumb-Dhindsa, P. and Thorpe, T.A. (1981) Leaf senescence: correlated with increased levels of membrane permeability and lipid peroxidation, and decreased levels of superoxide dismutase and catalase. *J. Exp. Bot.* 32: 93–101.

Di Baccio, D., Kopriva, S., Sebastiani, L. and Rennenberg, H. (2005) Does glutathione metabolism have a role in the defence of poplar against zinc excess? *New Phytol.* 167: 73–80.

Ebbs, S.D. and Kochian, L.V. (1997) Toxicity of zinc and copper to *Brassica* species: implications for phytoremediation. *J. Environ. Qual.* 26: 776–781.

Feechan, A., Kwon, E., Yun, B.W., Wang, Y., Pallas, J.A. and Loake, G.J. (2005) A central role for S-nitrosothiols in plant disease resistance. *Proc. Natl. Acad. Sci. USA* 102: 8054–8059.

Feigl, G., Kolbert, Z., Lehotai, N., Molnár, Á., Ördög, A., Bordé, Á., et al. (2016) Different zinc sensitivity of *Brassica* organs is accompanied by distinct responses in protein nitration level and pattern. *Ecotoxicol. Environ. Saf.* 125: 141–152.

Feigl, G., Lehotai, N., Molnár, Á., Ördög, A., Rodríguez-Ruiz, M., Palma, J.M., et al. (2015) Zinc induces distinct changes in the metabolism of reactive oxygen and nitrogen species (ROS and RNS) in the roots of two *Brassica* species with different sensitivity to zinc stress. *Ann. Bot.* 116: 613–625.

Frungillo, L., Skelly, M.J., Loake, G.J., Spoel, S.H. and Salgado, I. (2014) S-nitrosothiols regulate nitric oxide production and storage in plants through the nitrogen assimilation pathway. *Nat. Commun.* 5: 5401.

Galetskiy, D., Lohscheider, J.N., Kononikhin, A.S., Popov, I.A., Nikolaev, E.N. and Adamska, I. (2011) Phosphorylation and nitration levels of photosynthetic proteins are conversely regulated by light stress. *Plant Mol. Biol.* 77: 461–473.

Gallé, Á., Csiszár, J., Secenji, M., Guóth, A., Cseuz, L., Tari, I., et al. (2009) Glutathione transferase activity and expression patterns during grain filling in flag leaves of wheat genotypes differing in drought tolerance: response to water deficit. *J. Plant Physiol.* 166: 1878–1891.

Gow, A.J., Farkouh, C.R., Munson, D.A., Posencheg, M.A. and Ischiropoulos, H. (2004) Biological significance of nitric oxide-mediated protein modifications. *Am. J. Physiol. Lung Cell Mol. Physiol.* 287: L262–L268.

Griffith, O.W. (1980) Determination of glutathione and glutathione disulfide using glutathione reductase and 2-vinylpyridine. *Anal. Biochem.* 106: 207–211.

Guerra, D., Ballard, K., Truebridge, I. and Vierling, E. (2016) S-nitrosation of conserved cysteines modulates activity and stability of S-nitrosoglutathione reductase (GSNOR). *Biochemistry* 55: 2452–2464.

Gupta, B., Pathak, G.C. and Pandey, N. (2011) Induction of oxidative stress and antioxidant responses in *Vigna mungo* by zinc stress. *Russ. J. Plant Physiol.* 58: 85–91.

Helmersson, A., von Arnold, S. and Bozhkov, P.V. (2008) The level of free intracellular zinc mediates programmed cell death/cell survival decisions in plant embryos. *Plant Physiol.* 147: 1158–1167.

Holzmeister, C., Fröhlich, A., Sarioglu, H., Bauer, N., Durner, J. and Lindermayr, C. (2011) Proteomic analysis of defense response of wild type *Arabidopsis thaliana* and plants with impaired NO- homeostasis. *Proteomics* 11: 1664–1683.

Jahnová, J., Luhová, L. and Petřivalský, M. (2019) S-nitrosoglutathione reductase- the master regulator of protein S-nitrosation in plant NO signalling. *Plants* 8: 48.

Jain, P. and Bhatla, S.C. (2018) Molecular mechanisms accompanying nitric oxide signalling through tyrosine nitration and S-nitrosylation of proteins in plants. *Funct. Plant Biol.* 45: 70–82.

Jain, R., Srivastava, S., Solomon, S., Shrivastava, A.K. and Chandra, A. (2010) Impact of excess zinc on growth parameters, cell division, nutrient accumulation, photosynthetic pigments and oxidative stress of sugarcane (*Saccharum* spp.). *Acta Physiol. Plant.* 32: 979–986.

Kato, M. and Shimizu, S. (1987) Chlorophyll metabolism in higher plants. VII. Chlorophyll degradation in senescing tobacco leaves; phenolic-dependent peroxidative degradation. *Can. J. Bot.* 65: 729–735.

Kiekens, L. (1995) Zinc. *In* Heavy Metals in Soils. Edited by Alloway, B.J. pp. 284–305. Blackie Academic and Professional, London.

Kneeshaw, S., Gelineau, S., Tada, Y., Loake, G.J. and Spoel, S.H. (2014) Selective protein denitrosylation activity of thioredoxin-h5 modulates plant immunity. *Mol. Cell* 56: 153–162.

Kolbert, Z., Feigl, G., Bordé, Á., Molnár, Á. and Erdei, L. (2017) Protein tyrosine nitration in plants: present knowledge, computational prediction and future perspectives. *Plant Physiol. Biochem.* 113: 56–63.

Kolbert, Z., Pető, A., Lehotai, N., Feigl, G., Ördög, A. and Erdei, L. (2012) *In vivo* and *in vitro* studies on fluorophore-specificity. *Acta Biol. Szeged* 56: 37–41.

Kovács, I., Holzmeister, C., Wirtz, M., Geerlof, A., Fröchlich, T. and Römling, G. (2016) ROS-mediated inhibition of S-nitrosoglutathione reductase contributes to the activation of anti-oxidative mechanisms. *Front. Plant Sci.* 7: 1669.

Kwon, E., Feechan, A., Yun, B.W., Hwang, B.H., Pallas, J.A., Kang, J.G., et al. (2012) AtGSNOR1 function is required for multiple developmental programs in *Arabidopsis*. *Planta* 236: 887–900.

Lamotte, O., Bertoldo, J.B., Besson-Bard, A., Rosnoblet, C., Aimé, S., Hichami, S., et al. (2015) Protein S-nitrosylation: specificity and identification strategies in plants. *Front. Chem.* 2: 114.

Lee, U., Wie, C., Fernandez, B.O., Feelisch, M. and Vierling, E. (2008) Modulation of nitrosative stress by S-nitrosoglutathione reductase is critical for thermotolerance and plant growth in *Arabidopsis*. *Plant Cell* 20: 786–802.

Lehotai, N., Kolbert, Z., Peto, A., Feigl, G., Ordog, A., Kumar, D., et al. (2012) Selenite-induced hormonal and signalling mechanisms during root growth of *Arabidopsis thaliana* L. *J. Exp. Bot.* 63: 5677–5687.

Li, X., Yang, Y., Jia, L., Chen, H. and Wei, X. (2013) Zinc-induced oxidative damage, antioxidant enzyme response and proline metabolism in roots and leaves of wheat plants. *Ecotoxicol. Environ. Saf.* 89: 150–157.

Lindermayr, C. (2018) Crosstalk between reactive oxygen species and nitric oxide in plants: key role of S-nitrosoglutathione reductase. *Free Rad. Biol. Med.* 122: 110–115.

Lucini, L. and Bernardo, L. (2015) Comparison of proteome response to saline and zinc stress in lettuce. *Front. Plant Sci.* 6: 240.

Monnet, F., Vaillant, N., Vernay, P., Coudret, A., Sallanon, H. and Hitmi, A. (2001) Relationship between PSII activity, CO₂ fixation, and Zn, Mn and Mg contents of *Lolium perenne* under zinc stress. *J. Plant Physiol.* 158: 1137–1144.

Morina, F., Jovanovic, L., Mojovic, M., Vidovic, M., Pankovic, D. and Veljovic Jovanovic, S. (2010) Zinc-induced oxidative stress in *Verbascum thapsus* is caused by an accumulation of reactive oxygen species and quinhydrone in the cell wall. *Physiol. Plant.* 140: 209–224.

Nakano, Y. and Asada, K. (1981) Hydrogen peroxide is scavenged by ascorbate specific peroxidase in spinach chloroplasts. *Plant Cell Physiol.* 22: 867–880.

Nouet, C., Motte, P. and Hanikenne, M. (2011) Chloroplastic and mitochondrial metal homeostasis. *Trends Plant Sci.* 16: 395–404.

Noulas, C., Tziouvalekas, M. and Karyotis, T. (2018) Zinc in soils, water and food crops. *J. Trace Elem. Med. Biol.* 49: 252–260.

Papdi, C., Ábrahám, E., Joseph, M.P., Popescu, C., Koncz, C. and Szabados, L. (2008) Functional identification of *Arabidopsis* stress regulatory genes using the controlled cDNA overexpression system. *Plant Physiol.* 147: 528–542.

Pető, A., Lehotai, N., Feigl, G., Tugyi, N., Ördög, A., Gémes, K., et al. (2013) Nitric oxide contributes to copper tolerance by influencing ROS metabolism in *Arabidopsis*. *Plant Cell Rep.* 32: 1913–1923.

Prats, E., Carver, T.L.W. and Mur, L.A.J. (2008) Pathogen-derived nitric oxide influences formation of the appressorium infection structure in the phytopathogenic fungus *Blumeria graminis*. *Res. Microbiol.* 159: 476–480.

Ramakrishna, B. and Rao, S.S. (2015) Foliar application of brassinosteroids alleviates adverse effects of zinc toxicity in radish (*Raphanus sativus* L.) plants. *Protoplasma* 252: 665–677.

Rouached, H. (2013) Recent developments in plant zinc homeostasis and the path toward improved biofortification and phytoremediation programs. *Plant Signal. Behav.* 8: e22681.

Sagardoy, R., Morales, F., López-Millán, A.F., Abadía, A. and Abadía, J. (2009) Effects of zinc toxicity on sugarbeet (*Beta vulgaris* L.) plants grown in hydroponic. *Plant Biol. (Stuttg)* 11: 339–350.

Sakamoto, A., Ueda, M. and Morikawa, H. (2002) *Arabidopsis* glutathione-dependent formaldehyde dehydrogenase is an S-nitrosoglutathione reductase. *FEBS Lett.* 515: 20–24.

Sawa, T., Akaike, T. and Maeda, H. (2000) Tyrosine nitration by peroxynitrite formed from nitric oxide and superoxide generated by xanthine oxidase. *J. Biol. Chem.* 275: 32467–32474.

Schützendübel, A. and Polle, A. (2002) Plant responses to abiotic stresses: heavy metal-induced oxidative stress and protection by mycorrhization. *J. Exp. Bot.* 53: 1351–1365.

Sharma, S.K., Goloubinoff, P. and Christen, P. (2008) Heavy metal ions are potent inhibitors of protein folding. *Biochem. Biophys. Res. Commun.* 372: 341–345.

Tewari, R.K., Kumar, P. and Sharma, P.D. (2008) Morphology and physiology of zinc stressed mulberry plants. *J. Plant Nutr. Soil Sci.* 171: 286–294.

Thompson, J.W., Forrester, M.T., Moseley, M.A. and Foster, M.W. (2013) Solid-phase capture for the detection and relative quantification of S-nitrosoproteins by mass spectrometry. *Methods* 62: 130–137.

Umbreen, A., Lubega, J., Cui, B., Pan, Q., Jiang, J. and Loake, G.J. (2018) Specificity of nitric oxide signalling. *J. Exp. Bot.* 19: 3439–3448.

van der Vliet, A., Eiserich, J.P., Shigenaga, M.K. and Cross, C.E. (1999) Reactive nitrogen species and tyrosine nitration in the respiratory tract: epiphenomena or. *Am. J. Respir. Crit. Care Med.* 160: 1–9.

Wang, C., Zhang, S.H., Wang, P.F., Hou, J., Zhang, W.J., Li, W., et al. (2009) The effect of excess Zn on mineral nutrition and antioxidative response in rapeseed seedlings. *Chemosphere* 75: 1468–1476.

Weckx, J.E.J. and Clijsters, H.M.M. (1997) Zn phytotoxicity induces oxidative stress in primary leaves of *Phaseolus vulgaris*. *Plant Physiol. Biochem.* 35: 405–410.

Welinder, C. and Ekblad, L. (2011) Coomassie staining as loading control in Western blot analysis. *J. Proteome Res.* 10: 1416–1419.

Wiśniewski, J.R., Zougman, A., Nagaraj, N. and Mann, M. (2009) Universal sample preparation method for proteome analysis. *Nat. Methods* 6: 359–362.

Xu, J., Yin, H., Li, Y. and Liu, X. (2010) Nitric oxide is associated with long-term zinc tolerance in *Solanum nigrum*. *Plant Physiol.* 154: 1319–1334.

Xu, S., Guerra, D., Lee, U. and Vierling, E. (2013) S-nitrosoglutathione reductases are low-copy number, cysteine-rich proteins in plants that control multiple developmental and defense responses in *Arabidopsis*. *Front. Plant Sci.* 4: 430.

Yang, H., Mu, J., Chen, L., Feng, J., Hu, J., Li, L., et al. (2015) S-nitrosylation positively regulates ascorbate peroxidase activity during plant stress responses. *Plant Physiol.* 167: 1604–1615.

Zaffagnini, M., De Mia, M., Morisse, S., Di Giacinto, N., Marchand, C.H., Maes, A., et al. (2016) Protein S-nitrosation in photosynthetic organisms: a comprehensive overview with future perspectives. *Biochim. Biophys. Acta* 1864: 952–966.

Zarcinas, B.A., Ishak, C.F., McLaughlin, M.J. and Cozens, G. (2004) Heavy metals in soils and crops in Southeast Asia. *Environ. Geochem. Health* 26: 343–357.